

The Extrinsic Precursor Kinetics of Methane Adsorption onto Ethynylidyne-Covered Pt(111)

A. F. Carlsson and R. J. Madix*

Stanford University, Stanford, California 94305

Received: October 27, 2000; In Final Form: February 20, 2001

The kinetics of methane trapping on ethynylidyne-covered Pt(111) were investigated using supersonic molecular beam techniques at surface temperatures between the temperature at which methane desorbs from the monolayer and from a second layer. The inability of the Langmuir,¹ Kisliuk,² or modified Kisliuk^{3,4} models to fit the temperature dependence of the adsorption probability prompted the derivation of a model in which adsorption is forced through an extrinsic precursor. The difference in activation energies for desorption from the precursor state and migration of the extrinsic precursor, $E_d' - E_m'$, is 5.4 kJ/mol, and the ratio of preexponential factors, $k_d^{(0)}/k_m^{(0)}$, is 2×10^4 . The difference in activation energies suggests that the extrinsic precursor makes about 10^5 site hops near the desorption temperature in search of a binding site. The high degree of corrugation in the gas–surface potential may be responsible for the relatively high barrier to migration in the extrinsic precursor.

Introduction

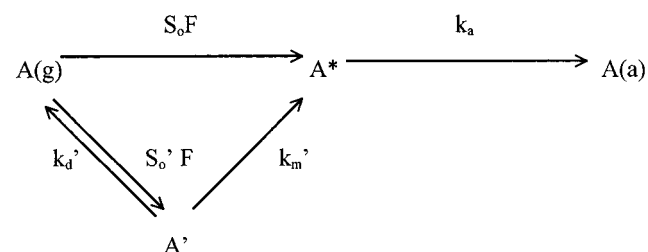
The adsorption of gases onto solid surfaces is a fundamental step in heterogeneous catalysis which merits quantitative description. Langmuir first proposed such a description by suggesting that the sticking probability is proportional to the number of free adsorption sites left on the surface;¹ the resulting sticking probability is $S = S_0(1 - \theta)$ where S_0 is the initial sticking probability on the clean surface, and θ is the fractional coverage. The inability of a simple site exclusion model to predict anything but a linearly decreasing sticking probability with coverage prompted Kisliuk^{2,5} to derive a probabilistic model which allows for adsorption on top of filled sites, assuming the trapping probability on filled or vacant sites to be the same. King and Wells⁶ derived a model for N₂ chemisorption on W(100) from a kinetic viewpoint which ended in the same result as the probabilistic model derived by Kisliuk.² Kang et al.³ and Arumainayagam et al.⁴ later modified the Kisliuk model to allow for different trapping probabilities on filled and vacant sites, based on the observation that the sticking probability of gases onto adsorbed layers was different than the sticking probability onto the clean surface; they also removed the channel which forced adsorption through a precursor on the bare surface before adsorption.

Before outlining methods for quantitatively describing the adsorption probability, we review the possible scenarios that may proceed during a gas–surface collision.⁶ An incident molecule may scatter back into the gas phase with or without energy loss, or lose sufficient translational energy to remain on the surface, perhaps in a transient state in which it migrates to a binding site. An adsorbed molecule may subsequently form a chemical bond with the surface, i.e., chemisorption, form a weak bond with the surface as a result of dispersion forces, i.e., physisorption, or desorb back into the gas phase. The initial transient state may occur on top of molecules which are already adsorbed on the surface (extrinsic precursor), or on the clean surface (intrinsic precursor). In the case of physisorption, where

no dissociation or strong chemical bond formation with the surface occurs, the intrinsic precursor state is not distinguishable from the state of physisorption unless the surface is energetically heterogeneous; e.g., it consists of terrace, edge, and kink sites of different binding energy. However, quasi-trapped states may form whose momentum component perpendicular to the surface is accommodated, whereas their parallel momentum is not. Higher surface temperatures allow mobile adsorbates to surmount the activation energy barrier to surface migration. If a chemisorption bond is to be formed, the energy released from the exothermicity of bond formation to the surface must also be dissipated.

These steps involving the thermalized precursors can be represented by the following kinetic scheme, normally referred to as the Kisliuk model:

SCHEME 1



where A(g) is the species A in the gas phase, A' is in the extrinsic precursor state, which is generally pictured to be a metastable state adsorbed upon an adsorbed species or at least strongly destabilized by adsorbed species, A* is the intrinsic precursor state, i.e., a molecularly adsorbed species, and A(a) is in the adsorbed state. S_0 is the sticking probability onto the clean surface, F is the flux, k_d' is the rate constant for desorption out of the extrinsic precursor state, S_0' is the sticking probability into the extrinsic precursor state, k_m' is the rate constant for conversion of the extrinsic precursor into the intrinsic precursor, and k_a is the rate constant for conversion of the intrinsic precursor to the final adsorbed state. In the case of molecular

* Author to whom correspondence should be addressed.

(associative) adsorption the intrinsic precursor A^* is generally replaced by the final adsorption state $A(a)$, and k_a is no longer relevant; this second scheme has been referred to as the modified Kisliuk model.^{3,4}

Using the Kisliuk model, as shown in Scheme 1 above, the sticking probability is

$$\frac{1}{F} \frac{dA(a)}{dt} = S(\theta) = \frac{S_o}{1 + \left\{ \frac{\theta}{1 - \theta} \right\} K} \quad (1)$$

with

$$S_o = \frac{\alpha k_a}{k_a + k_d'} \quad (2)$$

and

$$K = \left(\frac{k_a + k_d' + k_m}{k_a + k_d'} \right) \left(\frac{k_d'}{k_m' + k_d'} \right) \quad (3)$$

The Kisliuk model also assumes that the sticking probability into the intrinsic and extrinsic precursors is the same. Within this framework $S(\theta)$ either remains constant or decreases with coverage.

In contrast, the modified Kisliuk model^{3,4} yields

$$P_a \equiv \frac{1}{F} \frac{dA(a)}{dt} = S(\theta) = S_o(1 - \theta) + \frac{S_o'(1 - \theta)q_m\theta}{(1 - q_m\theta)} \quad (4)$$

where

$$q_m = \frac{k_m'}{k_d' + k_m'} \quad (5)$$

The sticking probability can increase with coverage, and trapped molecules are not forced to go through an intrinsic precursor before adsorption in the final state. Behavior consistent with the modified Kisliuk model has been observed for argon,⁷ xenon,⁸ methane,⁷ ethane,⁴ and neopentane⁹ adsorption on Pt(111), and ethane on Ir(110)-(1 × 2),³ where in all cases the trapping probability increases with increasing self-coverage. Although the general kinetic scheme of this model should hold for all molecular adsorption systems, we expect that the parameters involved will change for different metals and adsorbates, because the binding energies of A' and $A(a)$ will be different, and thus the k_i will differ.

Both molecular dynamics and Monte Carlo simulations have been used to describe molecular adsorption in its different stages. Stochastic trajectory calculations using an empirical Morse potential derived from measurements of ethane trapping on Pt(111) have been used to predict the initial trapping probabilities of methane and propane on Pt(111) and Pt(110)-(1 × 2)¹⁰ and *n*-butane, isobutane, and neopentane on Pt(111).¹¹ Simulation methods are accurate because they follow the adsorption process on a molecular level, but they require detailed information about the gas-surface potential, which currently can only be derived from experiment. Macroscopic kinetic schemes are still valuable because they provide an overall description of the adsorption process.

In this molecular beam study we focus our attention on methane trapping on ethylidyne-covered Pt(111) via the extrinsic precursor. Ethylidyne chemisorbs to the Pt(111) surface in a $p(2 \times 2)$ structure¹² and is stable for long periods, allowing a set of adsorption experiments to be performed on a reproducible

surface. The ethylidyne species are rigidly bound in 3-fold hollow site and cannot be easily displaced laterally by incident methane molecules. STM images of ethylidyne-saturated Pt(111)¹³ show a defect density of approximately 25%, even with observation of an ordered $p(2 \times 2)$ structure with LEED.

Experimental Section

The basic experimental apparatus used in this study has been described in detail elsewhere.¹⁴ Briefly, it consists of an ultrahigh vacuum chamber with a base pressure of 5×10^{-11} Torr coupled to a triply pumped supersonic molecular beam source. The main chamber is equipped with a rear view LEED/AES electron optics and two quadrupole mass spectrometers. The first mass spectrometer is mounted on a bellows and has a flow-through Fuelner cap^{15,16} on the ionizer; the hole in the cap can be placed 1 mm in front of the sample for selective detection of components desorbing from the surface. The second mass spectrometer can be rotated 180 degrees about the sample at a fixed radius of 10.5 cm and is used in conjunction with a lock-in amplifier and 50% duty beam chopper to measure the velocity of the molecules in the beam.

The Pt(111) crystal (10 mm diameter) was cleaned by cycles of Ar^+ sputtering and oxygen cleaning. When surface impurity concentrations were below the sensitivity of AES (<0.01 ML) and a sharp $p(1 \times 1)$ hexagonal LEED pattern was observed, the surface was assumed to be clean and well ordered. Typically only one cycle of oxygen cleaning was needed each day. The sample can be resistively heated with proportional, integral, and derivative (PID) control to 1200 K and cooled to 30 K using a liquid helium cryostat.¹⁷ Temperatures were measured to ± 0.5 K using 0.125 mm chromel and alumel thermocouple wires spot-welded to the back of the crystal and braided to 0.5 mm wires of the same type, which run up the manipulator to the feed-through to minimize offsets in the thermocouple voltage due to thermal gradients.¹⁸ Temperature calibrations at 5 K in liquid helium and 77 K in liquid nitrogen indicated that no corrections were needed to the thermocouple readings. The cooling time from 650 K to 30 K was approximately 12 min, allowing negligible adsorption from the background. In addition, TPD experiments were performed after cooling the sample to 30 K and letting a beam of methane strike the inert flag for the time needed to complete a dynamic trapping probability experiment (DTPE); no $m/z = 16, 18, 28, 32$, or 44 were detected up to 860 K. The primary background gases present during cooling at a total pressure of less than 3×10^{-10} Torr with the beam entering the chamber were H_2 , He, H_2O , CO, and CO_2 .

The molecular beam was formed by the supersonic expansion of gas through a monel nozzle that could be heated resistively with PID control to 750 K. The flux of molecules at the crystal was about $10^{14} s^{-1}$ on a $0.07 cm^2$ spot. Low energy beams (10 kJ/mol) were formed with pure CH_4 , whereas higher energy beams were formed by seeding CH_4 in He at various ratios and/or heating the nozzle. The method of King and Wells¹⁹ was used to measure direct sticking probabilities using a shutter in the beam source chamber and an inert, gold-plated flag in the main chamber. A reference signal was taken while the beam hit the inert flag and was compared to the transient drop in the partial pressure when CH_4 struck the surface and trapped, thus providing an initial trapping probability in the limit of zero coverage, as well as the trapping probability as a function of time while CH_4 accumulated on the surface. To ensure that the entire beam was impinging upon the crystal surface at each angle of incidence studied, a modulated helium beam was monitored with the rotatable mass spectrometer placed behind the crystal.

Surface coverages were measured using a calibrated leak system²⁰ consisting of a 426.7 mL stainless steel backing chamber with an MKS Baratron 121A pressure gauge attached to a 10 μ m pinhole leak gasket at the entrance to the main chamber. The area of the beam spot on the crystal was calibrated²¹ using the well-known coverage of CO on Pt(111) at 300 K²² and found to be 0.071 cm² in good agreement with predictions from the beam collimating geometry. The change in pressure of the backing chamber is related to the conductance of the pinhole leak by

$$c = -\frac{1}{P} \frac{dn}{dt} = \frac{V}{kT} \frac{d(\ln P/P_o)}{dt} \quad (6)$$

where c is the conductance, P is the pressure in the backing chamber, n is the number of molecules, t is time, V is the storage volume, k is Boltzmann's constant, and P_o is the initial pressure in the backing chamber. The calibrated conductance was then used to calculate the coverage on the surface during beam exposure using

$$F = \frac{l_b}{A_b} \quad (7)$$

$$\frac{l_b}{l_c} = \frac{V_b}{V_c} \quad (8)$$

$$\theta = \int_0^t FS(t) dt \quad (9)$$

where F is the flux, l_b is the leak rate of the beam, A_b is the area of the beam, l_c is the leak rate of the calibrated leak, V_b is the mass spec voltage due to the beam background, V_c is the mass spectrometer voltage due to the calibrated leak background, $S(t)$ is the net sticking probability as a function of time, and θ is the coverage.

Results

According to the modified Kisliuk model^{3,4}

$$P_a = \frac{R_a}{F} = \left[S_o' \left(\frac{k_m' \theta}{k_d' + k_m' (1 - \theta)} \right) + S_o \right] (1 - \theta) \quad (10)$$

or rearranged,

$$\left[\frac{P_a}{S_o' (1 - \theta)} - \frac{S_o}{S_o'} \right]^{-1} \theta - (1 - \theta) = \frac{k_d'}{k_m'} = \frac{k_d'^{(0)}}{k_m'^{(0)}} \exp \left[-\frac{(E_d - E_m)}{k_B T} \right] \quad (11)$$

where P_a is the net adsorption probability, R_a is the rate of adsorption, $k_i'^{(0)}$ is the pre-exponential factor for the rate constant k_i' , E_i' is the activation energy for the rate constant k_i' , k_B is the Boltzmann constant, T is the surface temperature, and θ is the fraction of the surface covered by adsorbate. The measured dependence of the trapping probability on temperature can thus be used to evaluate the ratio of preexponential factors and the difference in activation energies for desorption from the extrinsic precursor and conversion of the extrinsic precursor into a final binding state on the surface.

In a dynamic trapping probability experiment¹⁹ the net adsorption probability, P_a , is measured. If the surface temperature is selected so that there is no competing desorption, at

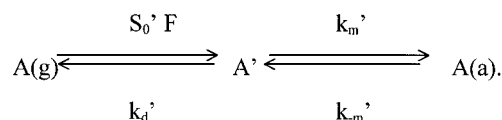
zero coverage the experiment yields directly the initial sticking probability S_o . If the surface temperature is sufficiently low that a second layer can be formed without competing desorption, the trapping probability into the extrinsic precursor state S_o' can also be obtained.¹⁷ Indeed, both of these values have been measured for methane trapping. The trapping probability of methane on clean Pt(111) at 50 K, 9 kJ/mol, and normal incidence, S_o , is 0.271.⁷ The trapping probability of methane on methane-covered Pt(111) at 30 K, 9 kJ/mol, and normal incidence, S_o' , is 0.980,¹⁷ and the trapping probability of methane on a combined methane and ethylidyne-saturated layer on Pt(111) at the same conditions is also $S_o' = 0.980$.²³

Using an initial value of the fraction of the total coverage, θ_{eth} , to be 0.50 for the ethylidyne adsorbate (the absolute coverage is 0.25 ML, which is half the coverage of the methane and ethylidyne-saturated surface) and $\theta_{CH_4} = 0$ corresponding to the initial trapping probability, it is apparent that certain measured adsorption probabilities, P_a , may give rise to a negative argument in the log term. Unfortunately, in the case of methane adsorption on the ethylidyne-covered surface, the argument of the log term does turn negative, suggesting that the modified Kisliuk model is inappropriate for describing the initial adsorption process.

The modified Kisliuk model assumes that an incoming molecule may adsorb into the extrinsic precursor or directly into its final adsorption state; further, the adsorption probability into the final state is proportional to the number of binding sites left, and the adsorption probability into the extrinsic precursor is proportional to the adsorbate coverage. In the case of methane adsorption onto an ethylidyne-covered Pt(111) surface, an incoming molecule may not be able to realize direct adsorption, and may be forced through an extrinsic precursor, due to the high ethylidyne coverage.

The "forced" precursor model is

SCHEME 2



Using this kinetic scheme and applying the kinetic steady-state approximation to $[A']$,

$$S_o' F + k_{-m}' [A] \theta_{eth} = k_d' [A'] + k_m' [1 - \theta] [A'] \quad \text{where } \theta = \theta_{eth} + \theta_{CH_4} \quad (12)$$

the net adsorption probability, P_a , onto the surface is found to be

$$P_a = \frac{R_a}{F} = \frac{S_o' k_m' (1 - \theta) - \frac{k_{-m}' k_d'}{F} \theta_{eth} [A]}{k_d' + k_m' (1 - \theta)} \quad (13)$$

where R_a is the net rate of adsorption ($d[A]/dt$), and F is the flux of molecules to the surface. The initial adsorption probability is given by

$$\lim_{\theta_{CH_4} \rightarrow 0} P_a = \frac{S_o' k_m' (1 - \theta_{eth})}{k_d' + k_m' (1 - \theta_{eth})} \quad (14)$$

or

$$\frac{S_o'}{P_a(\theta_{CH_4}=0)} - 1 = \frac{k_d'}{k_m'(1 - \theta_{eth})} = \frac{k_d^{(0)}}{k_m^{(0)}(1 - \theta_{eth})} \exp\left[\frac{-(E_d' - E_m')}{k_B T}\right] \quad (15)$$

This last form can be used to extract rate parameters from the dependence of the initial adsorption probability on temperature.

Measured Trapping Probability. The initial adsorption probability of methane incident with 9 kJ/mol kinetic energy at normal incidence on ethylidyne-covered Pt(111) is plotted against surface temperature in Figure 1. Between each measurement, the surface temperature was raised to 300 K to desorb methane, while keeping the ethylidyne structure intact. In addition, measurements were repeated at the end of the temperature sequence to ensure reproducibility. The net initial adsorption probability increases continuously from zero to 0.76 as the surface temperature is lowered from 70 K to 30 K.

For comparison, the adsorption probability near methane saturation on the ethylidyne-covered Pt(111) surface is also shown in Figure 1. Above a surface temperature of 56 K, the initial and saturation adsorption probabilities are identical, because too little methane accumulates on the surface to change the measured probability. Below the methane desorption temperature at 56 K the accumulation of methane on the surface facilitates trapping. At lower surface temperatures, more methane is stable on the surface, and the final trapping probability continues to increase, while the initial trapping probability does not change as significantly.

Representative dynamic trapping probability measurements (DTPEs) used to calculate the initial and final trapping probabilities are shown in Figure 2 for surface temperatures from 60 K to 34 K. Next to each DTPE is a temperature-programmed desorption (TPD) trace taken after beam exposure, which reflects the adsorption state of methane which accumulated on the surface during the beam exposure. For DTPEs conducted above 56 K, the corresponding TPD shows virtually no methane desorption, whereas desorption is detected below 56 K, indicating a stable state of adsorbed methane. Further decreases in the surface temperature increase the area of the 56 K TPD peak, until at 42 K, a second peak begins to form and develops fully when methane is dosed at 30 K. The DTPE at 30 K shows that methane adsorbs in multilayers at this temperature; indeed, the 35 K TPD peak continues to grow as the methane coverage increases. The formation of multilayers at 35 K suggests that the 56 K TPD peak is due to methane adsorption between ethylidyne molecules or at phase boundaries in the ordered ethylidyne adsorbate structure.

Forced Precursor Model Fit to Experimental Data. The expression for P_a (eq 15) predicts that $P_a = S_o'$ at low temperature, and is nearly independent of temperature, where $k_d' \ll k_m'(1 - \theta_{eth})$, and that there should be a significant temperature dependence at higher temperatures. The linear fit to the data above 56 K yields $E_d' - E_m' = 5.4$ kJ/mol and $k_d^{(0)}/k_m^{(0)}(1 - \theta_{eth}) = 4 \times 10^4$ (Figure 3). Assuming that ethylidyne saturates about half of the available surface sites, the ratio of preexponential factors becomes $k_d^{(0)}/k_m^{(0)} = 2 \times 10^4$. The extrinsic precursor, methane adsorbed on top of the ethylidyne-covered surface, desorbs at about 35 K, giving a rough estimate of the absolute value of the activation energy for desorption from the extrinsic precursor, E_d , as 9 kJ/mol,²⁴ assuming a preexponential factor of 5×10^{13} s⁻¹. The difference in activation energies for desorption from the extrinsic precursor

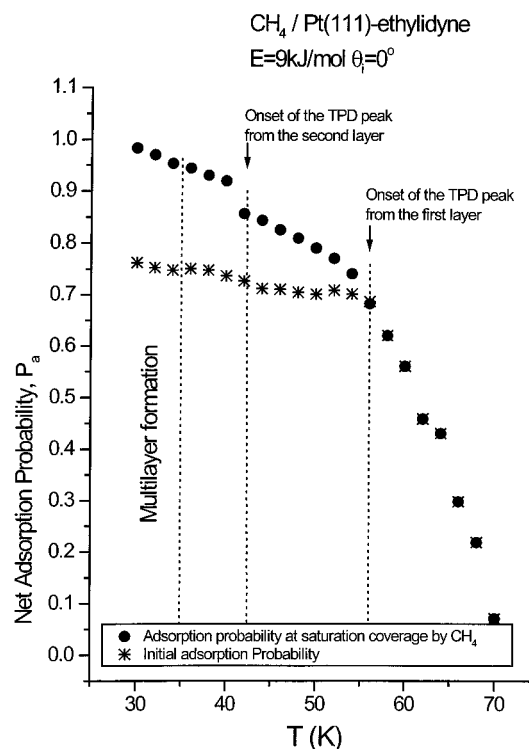


Figure 1. The initial trapping probability of CH₄ on Pt(111)-p(2x2)-CCH₃ (*) and on the methane-saturated ethylidyne (●)-covered Pt(111) as a function of surface temperature at normal incidence and 9 kJ/mol incident energy. The trapping probability on both surfaces is identical at surface temperature above 56 K, because the methane uptake is small and does not affect the trapping probability.

and migration from the extrinsic precursor to a binding site is about half the activation energy for desorption from the extrinsic precursor.

The temperature dependence of the adsorption probability confirms that migration from the extrinsic precursor to a binding site has a lower energy barrier than desorption. Near the desorption temperature both migration and desorption compete to deplete the concentration of the extrinsic precursor. When methane is adsorbed, the conversion from the bound state to the extrinsic precursor, k_{-m}' , is no longer negligible (eq 12). Above 56 K the reconversion of bound methane to the extrinsic precursor results in a greater net rate of desorption from the extrinsic precursor, and a smaller net adsorption probability is realized.

Methane Uptake. The steady-state uptake of methane on the surface must increase as the surface temperature is lowered, as is clearly shown by the integrated areas of the King and Wells traces. For the same flux and trapping probability into the extrinsic precursor, the desorption rate out of the extrinsic precursor decreases with decreasing temperature, allowing a higher flux into the adsorbed state from the extrinsic precursor. The steady-state uptake of methane during beam dosing as a function of surface temperature is shown in Figure 4. Each uptake measurement was calculated by integrating the time dependence of the methane partial pressure²⁰ during a dynamic adsorption probability experiment.¹⁹ The methane uptake is near zero at 70 K, and increases continuously with decreasing surface temperature; near 35 K methane multilayers begin to form and the uptake increases sharply. The activation energy for reconversion to the extrinsic precursor can be estimated using $E'_{-m} = E_d - E_d' + E_m'$ (Figure 5), resulting in $E'_{-m} = 10 \pm 2$ kJ/mol.

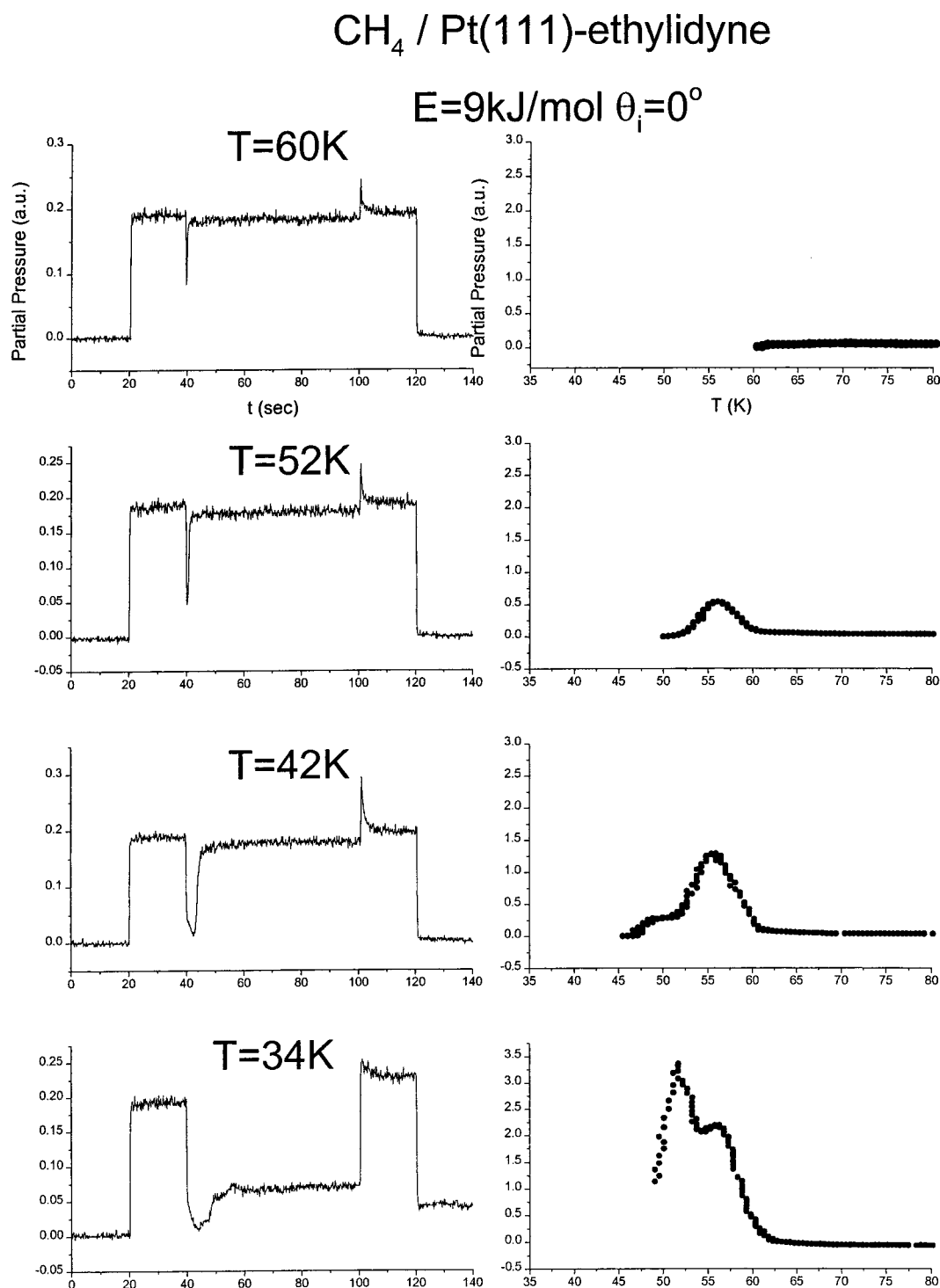


Figure 2. Example dynamic trapping probability experiments (DTPEs) of methane adsorption on ethynidyne-covered Pt(111) as a function of surface temperature with their respective temperature-programmed desorption (TPD) traces. Each DTPE was conducted at normal incidence and methane kinetic energy of 9 kJ/mol.

Discussion

A precursor model is required to describe the adsorption of alkanes^{3,4,9,17,21,23,25} and rare gases⁸ on metals because the trapping probability increases with increasing coverage, in contrast to the behavior predicted by the classical Langmuir site exclusion model.¹ In general, the enhanced trapping probability due to these weakly adsorbed species has been attributed to an increase in static corrugation of the gas-surface potential, which results in efficient interconversion of perpendicular and parallel momentum during a gas-surface collision.

The higher trapping probability on the adsorbate-covered surface results in adsorption through an extrinsic precursor, whereby incident molecules from the gas phase trap first on top of adsorbates before migrating to vacant binding sites. The adsorbed state which corresponds to the extrinsic precursor must be transient species if a second layer of the adsorbing species is not stable at the temperature of the surface; alternatively, molecules may remain adsorbed on top of adsorbates if the surface temperature is low enough for the rate of desorption from the extrinsic precursor, k'_d , to be small.

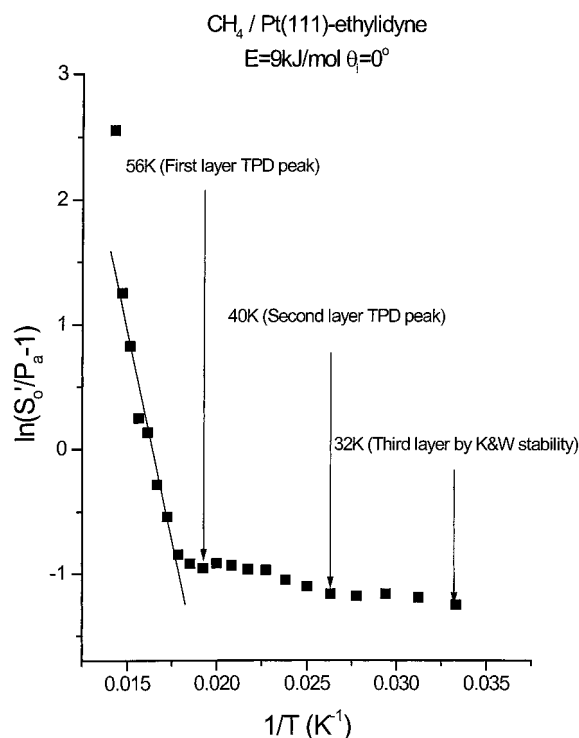


Figure 3. An Arrhenius plot using the forced precursor model, where incident molecules are forced to trap into the extrinsic precursor state before adsorbing. The model predicts a linear region at surface temperatures above 56 K, where the slope is the difference in activation energies for desorption and migration, and the intercept is the natural log of the ratio of pre-exponential factors for desorption and migration from the extrinsic precursor divided by the free site density.

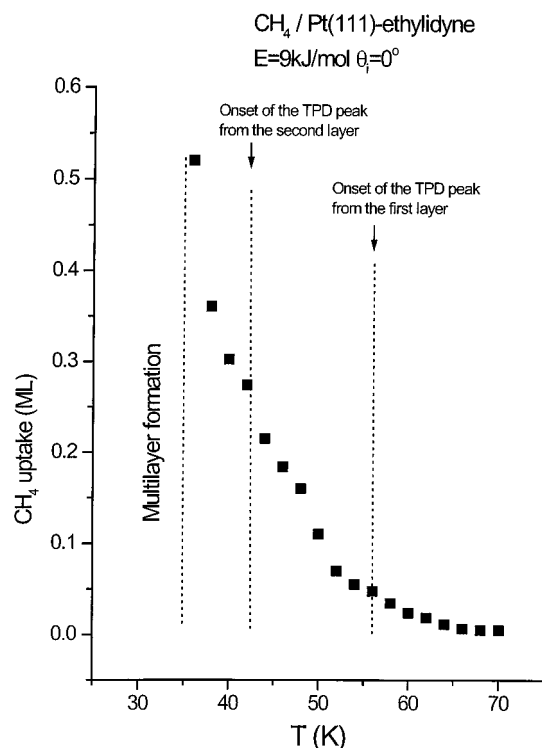


Figure 4. Methane uptake onto ethylidyne-covered Pt(111) as a function of surface temperature at normal incidence and 9 kJ/mol incident energy. The methane uptake reaches an asymptotic limit as multilayers begin to stabilize at 35 K.

The forced precursor model proposed to describe methane trapping on ethylidyne-covered Pt(111) may be somewhat

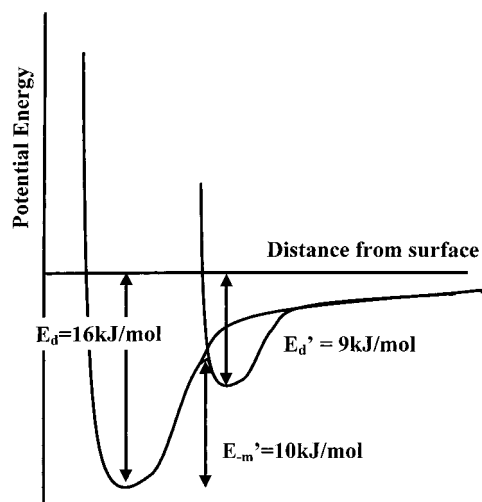


Figure 5. Potential energy curves for a molecule approaching a surface through an extrinsic precursor and into a bound state.

oversimplified. It is possible that methane may adsorb either above an ethylidyne or above an adsorbed methane before migration to the adsorbed state. However, a two-precursor model of this type is unnecessary for analysis of the initial adsorption probability, because on the time scale of the King and Wells measurement, the methane concentration is negligible compared to the ethylidyne concentration on the surface. Further, the trapping probability into the extrinsic precursor on top of ethylidyne and methane are both near unity for the energy examined, making it unnecessary to distinguish between them, even for the coverage analysis, at least to the first approximation.

The forced precursor model assumes that adsorbing molecules must first enter the extrinsic precursor before migrating to an adsorption site of lowest binding energy, or simply adsorb on top of adsorbates if the surface temperature is low enough. Our reasoning for assuming such a model was based on the relative areas free for adsorption and the trapping probability of methane on the clean surface compared to the ethylidyne-covered surface. The saturation coverage of methane on the clean Pt(111) surface at 50 K is 0.237 ML,¹⁷ compared to an ethylidyne coverage of 0.25 ML, where each ethylidyne adsorbate terminates in a methyl group. Further, the van der Waals radius of methane is 1.89 Å²⁶ and the covalent radius of Pt is 1.3 Å;²⁶ taking the van der Waals radius of an ethylidyne adsorbate to be the same as methane leaves only 1.42 Å available for methane adsorption between ethylidyne adsorbates suggesting that there is little chance for methane to directly strike an unoccupied site. Even in the event that an incident methane molecule hit a defect in the ethylidyne structure, the trapping probability on clean Pt(111) is much less than the trapping probability for a methane molecule which strikes an ethylidyne adsorbate. It is reasonable to assume that the combination of these two factors mitigates against the channel for direct adsorption.

The ratio of preexponential factors for desorption and migration to a bidding site gives further insight into the behavior of the extrinsic precursor when considered in the context of site to site diffusion. For surface diffusion (migration),

$$D = D_0 e^{-E_{diff}/RT} \quad (16)$$

where D is the diffusion rate constant, D_0 the diffusivity, and E_{diff} the activation energy for diffusion. The diffusivity is related to the attempt frequency for hopping by

$$D_o = \frac{1}{4} a^2 \nu \quad (17)$$

where a is the length of each hop, and ν is the attempt frequency.²⁷ From transition state theory,²⁸ we expect the attempt frequency to be $<10^{12}$, which, taking the hop length to be approximately 3 Å, yields a value of D_o of about 10^{-4} cm² s⁻¹.

There is a difference between the rate constants for diffusion of a precursor and that for its migration to a binding site. The attempt frequency for diffusion pertains to movement to the next lattice site, whereas the frequency factor for precursor migration describes conversion to the binding site. It is unlikely that on a given hop the binding site will be found at the next lattice site. For the extrinsic precursor of CH₄ migrating to defect sites we can write

$$k_m^{(0)'} = P\nu \quad (18)$$

where $k_m(0)'$ is the frequency of finding a binding site; i.e., the conversion rate constant, P is the probability of finding a binding site on the next hop, and ν is the attempt frequency for hopping to the next site. For a CH₄ molecule randomly placed on a lattice with a fraction of available sites $1/X_d$, the probability of being located next to an available site is $1/X_d$:

$$P = \frac{1}{X_d} \text{ (random placement)} \quad (19)$$

The defect density is not necessarily equal to the available site density for adsorption, because CH₄ molecules may not be able to bind at every defect in the ethynylidyne overlayer.

The ratio of rate constants, $k_d^{(0)}/k_m^{(0)} = 2 \times 10^4$, taken together with eq 18 and assuming $k_d(0)$ to be 10^{12} s⁻¹ suggests that $P = 5 \times 10^{-3}$. STM images of the Pt(111)-ethynylidyne surface^{29,13} show a larger density of defects in the ordered structure of ethynylidyne. Land et al.²⁹ observed well-ordered adsorbed ethylene with STM at 160 K and annealed the surface to 350 K to allow the reaction to form ethynylidyne. After cooling to 180 K they¹³ observed a well-ordered $p(2 \times 2)$ LEED pattern indicating long-range order, but observed a disordered local structure with STM. Despite the apparent defect density of approximately 25%, methane molecules in the extrinsic precursor appear to find only one in every 200 sites suitable for binding to the clean surface. In their ordered structure, ethynylidyne molecules occupy every other 3-fold hollow site to form a $p(2 \times 2)$ structure, and a defect often constitutes a spacing of three sites rather than two. It is possible that methane molecules require more space between ethynylidyne adsorbates to bind initially with the Pt(111) substrate. We also note that there is some uncertainty in the value of the preexponential factor for the desorption of methane that affects these estimates.

However, the saturation coverage of methane on the ethynylidyne-covered surface is about 0.2 ML, indicating that methane is ultimately able to adsorb in the vacancies between ethynylidyne adsorbates. The low probability of methane finding a suitable binding site is therefore due not to the scarcity of binding sites, but the low probability of conversion to its initial binding site. The apparent probability of conversion to this bound state, is about 5×10^{-3} , according to the analysis of preexponential factors above. This low probability suggests that the conditions of the trajectory must be specific in order for methane in the extrinsic precursor to be able to drop down into the physisorption well without converting back to the extrinsic precursor. Further, methane molecules which do make it into the physisorption well may find it difficult to lose enough energy to stay there before

reconverting to the extrinsic precursor. Furthermore, methane may have to migrate to its ultimate binding site to larger defects of low concentration into which it is more easily accommodated.

The distance traveled by the extrinsic precursor before desorption or conversion to a bound state is governed by the difference in the rates of desorption and migration. Gomer³⁰ has approximated the distance traveled using the expression

$$E_d' - E_m' = RT \ln \left(\frac{\langle x^2 \rangle^{1/2}}{a} \right) \quad (20)$$

where E_d' is the activation energy for desorption from the precursor, E_m' is the diffusion barrier, a is the root-mean-square jump distance, $\langle x^2 \rangle^{1/2}$ is the root mean distance traveled, and the average number of hops made by the precursor is $\langle x^2 \rangle^{1/2}/a$. For some systems, the number of hops may be quite large; for O₂ on oxygen-covered W, $E_m' = 4$ kJ/mol, and $E_d' = 12$ kJ/mol,³¹ suggesting that at 300 K, the extrinsic precursor has up to about 600 hops over filled sites to find a binding site. The difference in activation barriers is smaller for methane adsorption on ethynylidyne-covered Pt(111), where $E_d' - E_m' = 5.4$ kJ/mol, suggesting that at 300 K, the precursor only makes about 9 hops over filled sites before desorbing. However, below the desorption temperature, at 50 K, methane may make as many as 4×10^5 site hops.

The difference in activation energies for desorption and migration from the extrinsic precursor for methane adsorbing on ethynylidyne-covered Pt(111) suggests that the activation energy for migration, or the diffusion barrier, is not negligible compared with the activation energy for desorption from the precursor, and limits site hopping during the lifetime of the extrinsic precursor. The trapping of methane on ethynylidyne-covered Pt(111)²³ depends on the incident methane energy but not on the incident angle, resulting in total energy scaling. The lack of angular dependence in trapping suggests a highly corrugated gas-surface potential, which may be responsible for the diffusion barrier in the extrinsic precursor. Just as a corrugated gas-surface potential facilitates the interconversion of perpendicular to parallel momentum in the collision of a gas molecule with the surface, the corrugation may also hinder lateral motion of methane in the extrinsic precursor. Further, the gas-surface potential corrugation may facilitate conversion of parallel momentum to perpendicular momentum along the reaction channel toward desorption.

Conclusions

Methane adsorption on ethynylidyne-covered Pt(111) can be quantitatively described using a kinetic model which forces adsorbing molecules through an extrinsic precursor, from which they may desorb or migrate to binding sites on the surface. Experimental measurements of the trapping probability as a function of surface temperature suggest that the difference in barrier heights between desorption and migration from the extrinsic precursor is 5.4 kJ/mol, and the precursor makes about 10^5 site hops near the desorption temperature before adsorbing or desorbing. In general, an extrinsic precursor further from the surface will have a larger barrier to migration into the adsorbed state. The high degree of corrugation in the gas-surface potential evident from the angular dependence of the trapping probability²³ may also contribute to the relatively high barrier to migration from the extrinsic precursor. The activation energy for migration from the adsorbed state to the extrinsic precursor is estimated to be 10 kJ/mol.

Acknowledgment. We gratefully acknowledge the Department of Energy, Chemical Sciences Division, Office of Basic Energy Sciences (Grant DE-FG03-86ER13468) for financial support of this work.

References and Notes

- (1) Roberts, M. W.; McKee, C. S. *Chemistry of the Metal-Gas Interface*; Oxford University Press: Oxford, 1978.
- (2) Kisliuk, P. *J. Phys. Chem. Solids* **1957**, *3*, 95.
- (3) Kang, H. C.; Mullins, C. B.; Weinberg, W. H. *J. Chem. Phys.* **1990**, *92*, 1397.
- (4) Arumainayagam, C. R.; McMaster, M. C.; Madix, R. J. *J. Phys. Chem.* **1991**, *95*, 2461.
- (5) Kisliuk, P. *J. Phys. Chem. Solids* **1958**, *5*, 78.
- (6) King, D. A.; Wells, M. G. *Proc. R. Soc. London A* **1974**, *339*, 245.
- (7) Carlsson, A. F.; Madix, R. J. *Surf. Sci.* **2000**, *458*, 91–105.
- (8) Arumainayagam, C. R.; Stinnett, J. A.; McMaster, M. C.; Madix, R. J. *J. Chem. Phys.* **1991**, *95*, 5437.
- (9) Weaver, J. F.; Ho, K. L.; Krzyzowski, M. A.; Madix, R. J. *Surf. Sci.* **1998**, *400*, 11.
- (10) Stinnett, J. A.; Madix, R. J. *J. Chem. Phys.* **1996**, *105*, 1609.
- (11) Weaver, J. F.; Madix, R. J. *J. Chem. Phys.* **1999**, *110*, 10585.
- (12) Steininger, H.; Ibach, H.; Lehwald, S. *Surf. Sci.* **1982**, *117*, 685.
- (13) Land, T. A.; Michely, T.; Behm, R. J.; Hemminger, J. C.; Comsa, G. *J. Chem. Phys.* **1992**, *97*, 6774.
- (14) D'Evelyn, M. P.; Hamza, A. V.; Gdowski, G. E.; Madix, R. J. *Surf. Sci.* **1986**, *167*, 451.
- (15) Feulner, P.; Menzel, D. *J. Vac. Sci. Technol.* **1980**, *17*, 662.
- (16) Feulner, P.; Menzel, D. *J. Surf. Sci.* **1985**, *154*, 465.
- (17) Carlsson, A. F.; Madix, R. J. *J. Phys. Chem.*, in press.
- (18) Schlichting, H.; Menzel, D. *Rev. Sci. Instrum.* **1993**, *64*, 2013.
- (19) King, D. A.; Wells, M. G. *Surf. Sci.* **1972**, *29*, 454.
- (20) Yates, J. T. *Experimental innovations in surface science: a guide to practical laboratory methods and instruments*; Springer: New York, 1998.
- (21) Weaver, J. F.; Ikai, M.; Carlsson, A. F.; Madix, R. J. *Surf. Sci.*, in press.
- (22) Norton, P. R.; Davies, J. A.; Jackman, T. E. *Surf. Sci.* **1982**, *122*, L593.
- (23) Carlsson, A. F.; Madix, R. J. *Surf. Sci.*, in press.
- (24) Redhead, P. A. *Vacuum* **1962**, *12*, 203.
- (25) Carlsson, A. F.; Madix, R. J. *Surf. Sci.*, submitted.
- (26) Bondi, A. *J. Phys. Chem.* **1964**, *68*, 441.
- (27) Gomer, R. Surface Diffusion: Theoretical Aspects. In *Surface Mobilities on Solid Materials*; Binh, V. T., Ed.; Plenum Press: New York, 1981; Vol. 86, p 7.
- (28) Gomer, R. Microscopic Theories of D at Zero Coverage. In *Surface Mobilities on Solid Materials*; Binh, V. T., Ed.; Plenum: New York, 1981; Vol. 86, p 15.
- (29) Land, T. A.; Michely, T.; Behm, R. J.; Hemminger, J. C.; Comsa, G. *Appl. Phys. A* **1991**, *53*, 414.
- (30) Gomer, R. *Disc. Faraday Soc.* **1959**, *28*, 23.
- (31) King, D. A. *J. Vac. Sci. Technol.* **1980**, *17*, 241.